ACS Macro Letters

Letter

pubs.acs.org/macroletters

Buckminsterfullerene: A Strong, Covalently Bonded, Reinforcing Filler and Reversible Cross-Linker in the Form of Clusters in a Polymer

Junchun Yu,[†] Mingguang Yao,[‡] Gerhard Gröbner,[§] Bertil Sundqvist,[†] Bounphanh Tonpheng,[†] Bingbing Liu,[‡] and Ove Andersson*[,†]

[†]Department of Physics, Umeå University, 90187 Umeå, Sweden

[‡]State Key Laboratory of Superhard Materials, Jilin University, 130012, Changchun, China

[§]Department of Chemistry, Umeå University, 90187 Umeå, Sweden

Supporting Information

ABSTRACT: A Buckminsterfullerene/polyisoprene (C_{60}/PI) composite was synthesized at high-temperature, high-pressure (HP&HT) conditions. The composite has significantly improved tensile strength and Young's modulus, by up to 49% and 88% per wt % C_{60}, respectively, which is much higher than for corresponding composites with carbon nanotube (CNT) fillers. The reinforcing action of C_{60} fillers is different from that of CNTs as C_{60} becomes covalently bonded to PI chains, and C_{60} clusters in PI form C_{60}–C_{60} covalent bonds. The latter are reversible and break by heating at 1 bar, which suggests improved recyclability of the material and indicates that carbon nanostructures can be used as strong reversible cross-linkers ("vulcanizers") in elastomers.

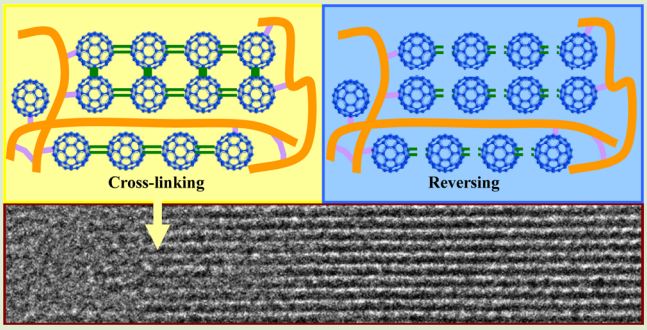

Nanostructured carbon materials such as graphene,[1] carbon nanotubes[2,3] (CNTs), and buckminsterfullerene[4] (C_{60}) attract much attention because of their great potential in nanotechnology.[5] C_{60} has been frequently tested as nanofiller in polymers, but because of its spherical shape, the potential usage is normally different from that of tubular-shaped CNTs and sheet-shaped graphene. The one- and two-dimensional structures of the latter are favorable for obtaining percolation networks at low filler contents and, thus, advantageous for imparting their transport properties to those of a composite material. Their geometries also assist load transfer in reinforcement applications. On the other hand, because of the 30 double bonds in its structure, C_{60} is more reactive and can therefore relatively easily form extended structures by generating new covalent bonds. By treatment under high-pressure, high-temperature (HP&HT) conditions or exposure to visible or ultraviolet light, double bonds on two adjacent C_{60} molecules can break and form a C_{60} dimer by [2 + 2] cycloaddition. The process proceeds by reaction with neighboring C_{60} molecules and typically gives polymeric, or at least oligomeric, C_{60}. A very interesting feature of C_{60} is that the transition into the polymeric (oligomeric) phase is reversible, and the original face-centered cubic (fcc) phase is recovered on heating to ~500 K near ambient pressure without decomposition of the C_{60} molecules.[6] This suggests that C_{60} clusters or oligomers can act as reversible, strongly reinforcing cross-linkers in, e.g., polymers. Here, we have exploited this feature to produce an elastomeric polymer which can be partly reversibly cross-linked into a state with significantly improved mechanical properties. This state, which was obtained purely by HP&HT treatment, shows 540% higher tensile strength (σ_{UTS}) and 900% higher Young's modulus (E) than neat polyisoprene (PI) produced at identical conditions. This improvement is significantly larger than the reinforcement achieved with multi-wall and single-wall carbon nanotube (MWCNT and SWCNT) fillers. Even more important, the observed partial reversibility indicates the feasibility of obtaining a fully recyclable state based on strongly reinforcing carbon nanostructured fillers.

Tensile stress–strain curves of recovered HP&HT treated C_{60}/PI (PIC) composites are shown in Figure 1a together with those of similarly treated PI,[7] SWCNT/PI,[7] and MWCNT/PI.[8] The samples of PI filled with 4.8 and 9.1 wt % C_{60} (denoted PIC5 and PIC9, respectively) were treated by pressurization to 1.5 GPa at room temperature, followed by isobaric heating to 513 K and finally annealing for 4 h at these conditions (see Experimental Section), at which PI becomes reactive and transforms from a liquid to a network (solid) polymer via a sluggish cross-linking process.[7,9] Moreover, under these conditions, neat C_{60} is known to polymerize into phases with orthorhombic or tetragonal structures.[10] As shown in Figure 1a,

Received: April 8, 2013
Accepted: May 22, 2013
Published: May 29, 2013

   dx.doi.org/10.1021/mz400171e | *ACS Macro Lett.* 2013, 2, 511–517

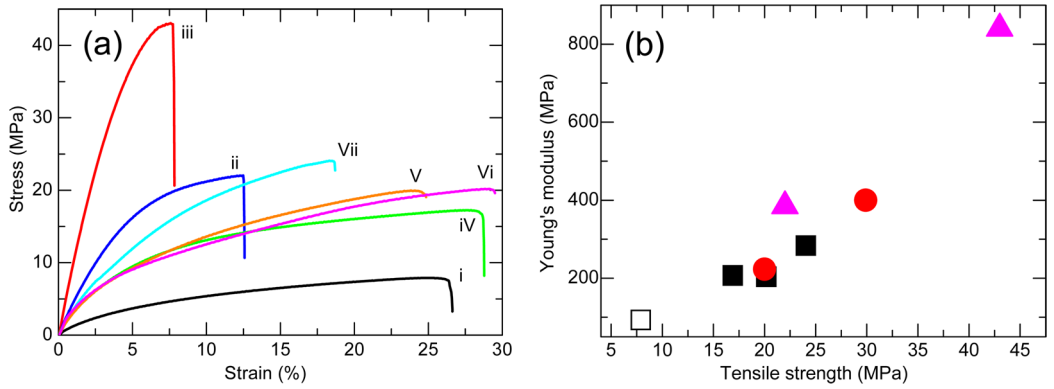

Figure 1. Tensile properties of HP&HT synthesized PI and PIC composites. (a) Stress−strain curves of: (i) PI from ref 7, (ii) PIC5, (iii) PIC9, (iv) PI + 5 wt % SWCNT from ref 7, (v) PI + 4.8 wt % P-MWCNT from ref 8, (vi) PI + 9.1 wt % F-MWCNT from ref 8, and (vii) PI + 9.1 wt % P-MWCNT from ref 8. (b) Tensile strength plotted against Young's modulus for: (□) PI from ref7, (■, red ●) P- and F-MWCNT composites from ref 8 and (pink ▲) PIC composites.

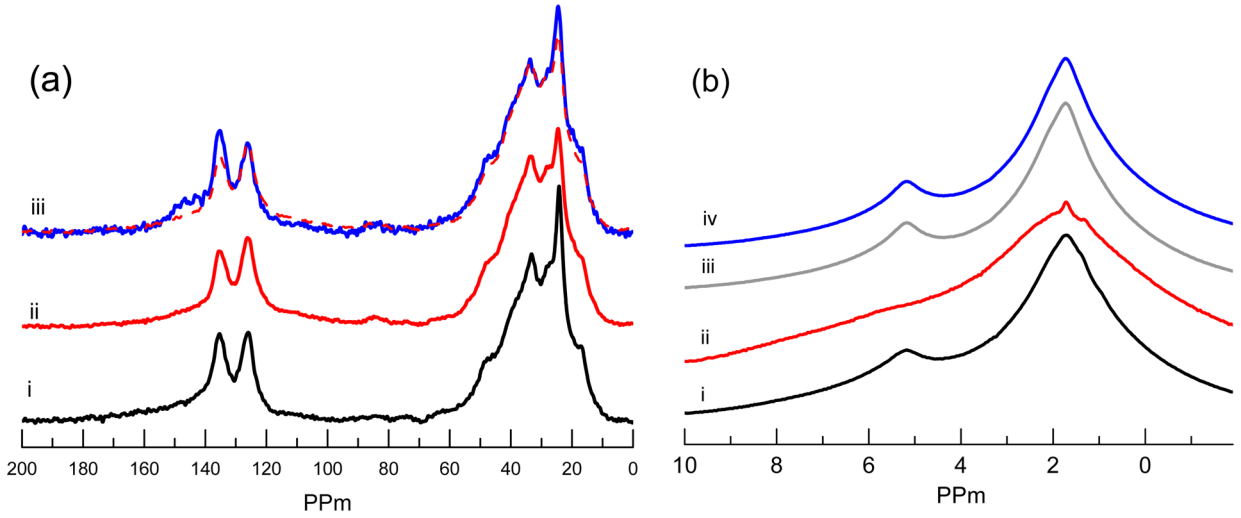

Figure 2. (a) Solid-state ^{13}C CP MAS NMR spectra for HP&HT treated samples at RT: (i) PI using a contact time of 1 ms duration and a repetition delay of 6 s at a MAS speed of 10 kHz, (ii) PIC9 using a contact time of 1 ms duration, and (iii) PIC9 using a contact time of 10 ms and a repetition delay of 6 s at a MAS speed of 10 kHz. The spectrum (ii) is shown with a dashed line with spectrum (iii) to highlight the signal from covalently bonded C_{60} near 143 ppm. (b) ^{1}H solid-state MAS NMR spectra at 10 kHz for HP&HT treated: (i) PI, (ii) PIC9, (iii) PI, and (iv) PIC9 after subsequent heat treatment at 450 K for 20 h under vacuum (see text).

both the σ_{UTS} and E of the PIC composites increase with increasing C_{60} content, but the tensile strain at break (ε_B) decreases. The σ_{UTS} of PIC5 and PIC9 are 280% and 540% higher, respectively, than that of PI treated at the same conditions.[7] The corresponding results for E are 410% and 900% times higher than that of PI.[7] The tensile stress−strain curves of the PIC composites show rather brittle behavior[11] with small ε_B (~10%), though not very different from that of PI (~25%) and CNT/PI composites.[7] It is also obvious that the C_{60}-filled PI shows higher σ_{UTS} and E than PI samples with the same amounts of nonfunctionalized MWCNTs[8] (P-MWCNT), functionalized MWCNTs[8] (F-MWCNT), or SWCNTs of about 1 μm length[7] and, respectively, 10, 10, and 1.4 nm diameter (Figure 1b), as well as carbon black (Supporting Information).

The behavior of the PIC composites is different from that of CNT-filled PI, which shows lower reinforcement but longer extension at break. In fact, addition of CNTs in PI improves the extension at break up to about 5 wt % CNT content.[7,8] The improved extension can be linked to a CNT-induced disruption of the chemical cross-link density,[7,8] which is the principal parameter determining the extension at break of neat PI. A high density of cross-links effectively limits the extension at break. Since the volume occupied by the CNTs, as well as the interphase in close vicinity of the CNTs, will be completely or partly deficient of cross-links,[8] this promotes flow and elongation of PI and thus better extension.

The tensile results and, in particular, the extensions at break thus suggest an explanation for the significantly better reinforcement of the PIC composites compared to the CNT composites. In CNT composites, the reinforcement depends critically on the dispersion achieved and on the load transfer between the matrix and the CNTs, which is supported by their high aspect ratio of ~10^2−10^3. CNTs typically interact with polymers noncovalently, even though there can be a closely coated/wrapped/bound polymer layer on CNTs[8] that appears to be augmented by high-pressure treatment.[7,8] Consequently, despite the large contact area between the matrix and the CNTs, it may still be insufficient to avoid CNT pull-out due to the weak CNT−polymer interfacial interaction.

The geometry and unsaturated structure of C_{60}, together with the decreased extension at break, suggest that the C_{60} filler

dx.doi.org/10.1021/mz400171e | ACS Macro Lett. 2013, 2, 511−517

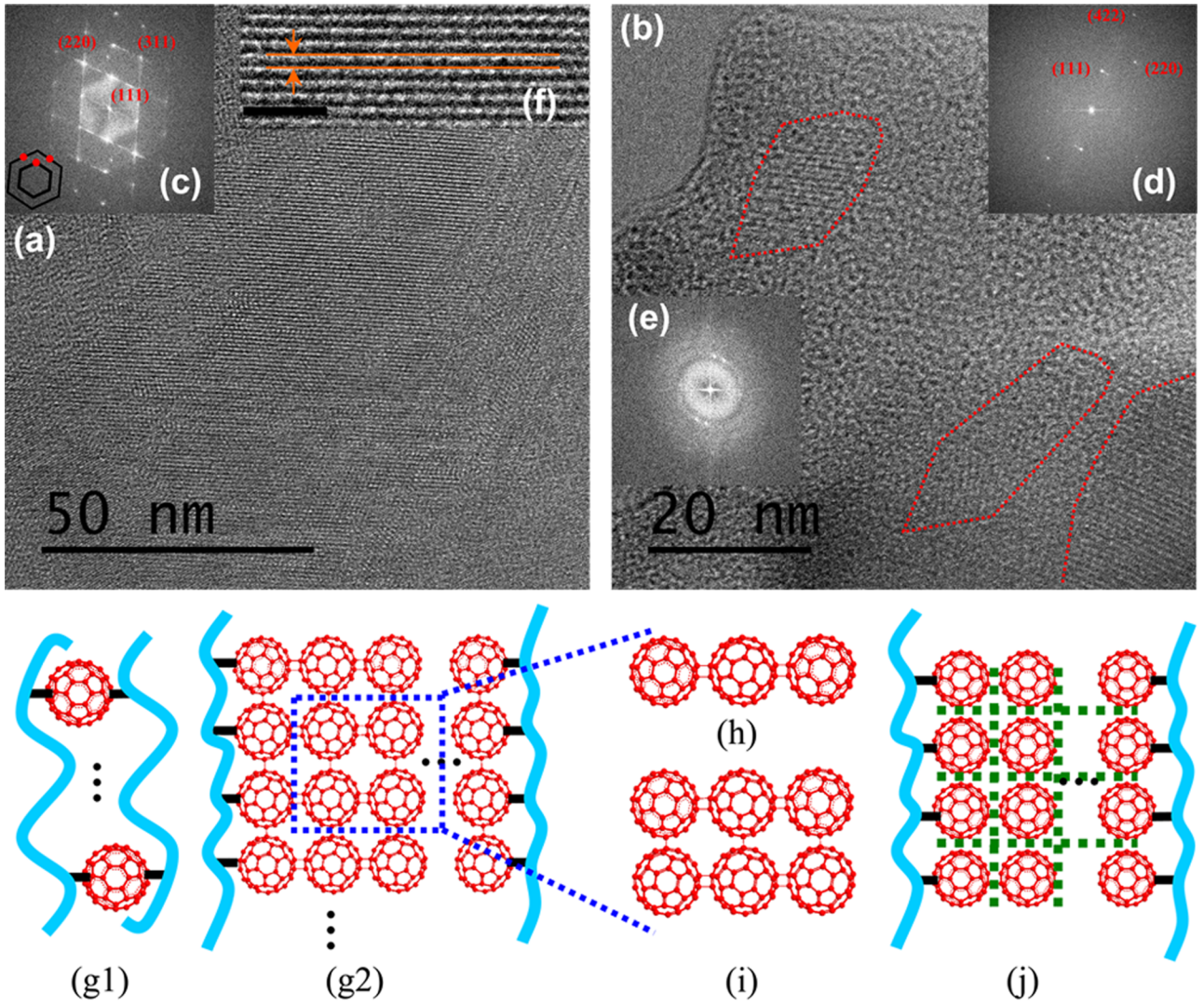

Figure 3. HRTEM of (a) HP&HT treated PIC9 sample; (b) HP&HT treated PIC9 sample after vacuum annealing; and (c) FFT image of the sample in (a), where the inset sketch clarifies the assignment positions. (d) and (e) are FFT images of the sample in (b). (f) A magnified view of a C_{60} crystal taken from (a), with a scale bar of 5 nm. Schematic model of the C_{60} microstructure in PI: (g1) C_{60} covalently bonded to PI and (g2) covalently bonded C_{60} clusters (polymeric C_{60}) after 1.5 GPa treatment. (h) and (i) are schematic plots of orthorhombic and tetragonal polymeric structure of C_{60}, respectively. (j) After vacuum annealing, the C_{60}−C_{60} bonds break, as highlighted by the dashed green lines. Note that PI−PI cross-links are not included in this sketch.

provides its strong reinforcement capability through a different mechanism than that of the CNTs. The CNT fillers are probably inert during the HP&HT treatment, at least those without functionalization. This means that they do not take part in the cross-linking reaction, and PI chains facing CNTs will have fewer cross-links than those in the bulk.[8] This cannot be the case for PIC composites. It is known that simply dispersing C_{60} in polymers can affect the chain mobility and change the glass transition temperature,[12,13] but C_{60} fillers do not normally provide much reinforcement and may even decrease σ_{UTS}, e.g., in polybutadiene−styrene raw rubber.[14] In another example, a 10 wt % C_{60}/polycaprolactone composite showed only 3% increase in σ_{UTS}, but a similar covalently bonded composite (polycaprolactone−NH_2 bonded with C_{60}−OH) showed 22% increase in σ_{UTS}.[15] The reinforcement obtained in the present study is more than an order of magnitude larger, but it has most likely a similar origin; i.e., it arises because C_{60} takes part in the HP&HT cross-linking process. The double bonds in C_{60} are available for covalent bonding both between C_{60} and PI and between neighboring C_{60} molecules in C_{60} clusters.

To investigate the changes caused by the HP&HT treatment, both PIC9 and PI were studied by solid-state ^{13}C cross-polarization magic angle spinning nuclear magnetic resonance (CP MAS NMR). Pure C_{60} has a single sharp resonance at 143 ppm in ^{13}C MAS NMR spectra.[16] However, the icosahedral symmetry (pseudospherical symmetry) of C_{60} is sensitive to its environment, and this can be probed by NMR.[17] For example, on the basis of splitting of the C_{60} resonance peak at 143 ppm, it was suggested that the presence of polymer causes a slight deviation from icosahedral symmetry for C_{60}.[18]

The ^{13}C NMR spectrum of untreated PI showed peaks with chemical shift values of 134.9, 125.5, 32.8, 27.0, and 23.9 ppm, as reported previously.[8,19] To observe possible covalent bonds between C_{60} and PI, we focused on the ^{13}C CP MAS NMR spectra of the samples. A CP pulse enables the detection of covalently bonded C_{60} atoms since this allows for magnetization transfer from close protons (−H) in the PI segment.

dx.doi.org/10.1021/mz400171e | ACS Macro Lett. 2013, 2, 511−517

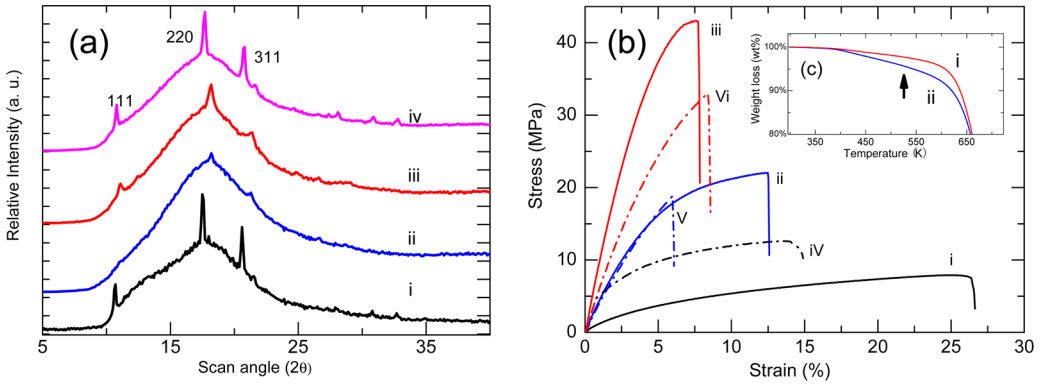

Figure 4. (a) WAXD spectra of PIC composites (from bottom to top): (i) untreated PIC9, (ii) HP&HT treated PIC5, (iii) HP&HT treated PIC9, (iv) HP&HT treated PIC9 after vacuum annealing. The curves are shifted vertically for clarity. (b) Stress–strain curves of as-recovered HP&HT synthesized PI and PIC composites: (i) PI from ref 7, (ii) PIC5 and (iii) PIC9; and stress–strain curves after vacuum annealing: (iv) PI, (v) PIC5, and (vi) PIC9. Inset (c): TGA traces of PIC samples: (i) PIC5 and (ii) PIC9.

Because of the lack of protons, "free" C_{60} or polymeric C_{60} would normally not show up under CP conditions in NMR spectra of PIC,[20,21] whereas C_{60} covalently bonded to PI should give a resonance near 143 ppm. If we first consider the measurements of PI and PIC9 using a MAS speed of 10 kHz and a contact time of 1 ms, the spectra shown in Figure 2a are almost identical with significantly broadened peaks consistent with highly cross-linked structures.[8] However, using a longer contact time of 10 ms for the PIC9 sample reveals a weak broad signal in the 141–151 ppm range (Figure 2a, iii), which thus coincides with the signal of C_{60}. (The results for HP&HT treated PI using 10 ms contact time showed no such feature.) The appearance of this broad resonance indicates that there is a magnetization transfer from a proton (–H) of PI to a carbon in C_{60} during the duration of the CP conditions, i.e., that C_{60} is covalently bonded to PI after the HP&HT treatment. Its occurrence only at long contact time is likely due to the long (C–H) interaction distance (Figure 3g). Thus, the NMR results suggest that double bonds in C_{60} break and form covalent bonds with PI, which occurs by a combination with the double bonds of PI or PI radicals. Peak area analyses of the NMR spectra[8] indicate that PIC9 had about 200% higher cross-link density than PI (Supporting Information). These covalent bonds formed during the HP&HT treatment provide one important link for the mechanical reinforcement of the PIC composites.

Moreover, the HP&HT treated PI and PIC9 samples were investigated by solid-state ^{1}H MAS NMR (Hahn-echo pulse experiment, rotor synchronized at 10 kHz spinning speed, Figure 2b). The ^{1}H MAS NMR spectrum suggests a more rigid structure in PIC9 (Figure 2b, ii) than in PI (Figure 2b, i). The spin–spin relaxation time (T_2) was 3.8×10^{-4} s (average) for PI but only 2.8×10^{-4} s (average) for PIC9. Before cross-linking, the T_2 value for the PIC9 composite was 1.7×10^{-3} s, and that of pure PI was 2.8×10^{-3} s. The strong decrease of T_2 due to the HP&HT treatment is associated with a reduced molecular mobility and suggests a higher degree of chemical cross-links in PIC9 than in pure PI. Cross-links restrain the segmental mobility, which besides an increase in T_2 relaxation rate also increases the glass transition temperature. Thus, this result also indicates that the glass transition of PIC9 is higher than that of pure PI, but this was not confirmed by direct measurements.

As mentioned, crystalline C_{60} can be cross-linked and form a polymeric structure after HP&HT treatment. To explore this possibility, the microstructure of the PIC9 composites was examined by high-resolution transmission electron microscopy (HRTEM, Figure 3) and wide-angle X-ray diffraction, (WAXD, Figure 4a). The WAXD spectrum of the untreated PIC9 sample shows several crystalline reflections superimposed on an amorphous halo, which is due to amorphous PI. The crystalline peaks, which occur at 10.7°, 17.5°, and 20.6°, are consistent with the reflections from the (111), (220), and (311) planes of crystalline C_{60} with fcc structure,[22,23] which shows that crystalline C_{60} existed in the amorphous PI matrix. After HP&HT treatment, the PIC9 sample exhibited a microstructure with a 2D partially crystalline feature (Figure 3a). Most of the C_{60} molecules appear well aligned and closely stacked into a fringe-like pattern, with a measured d spacing of 0.786 nm. We can identify individual C_{60} molecules in the crystalline domains (Figure 3f), which have a one-dimensional size of ~50 nm or less. The microstructure may be a mixture of mostly reacted (cross-linked) and unreacted (fcc) C_{60} and thus consists of fcc C_{60}, plus dimers, oligomers, and orthorhombic (Figure 3h) and/or tetragonal C_{60} polymers (Figure 3i). In the WAXD spectrum, the peak width of the crystalline peaks became larger, and the peaks became less distinct and slightly shifted to larger angles (11.1°, 18.2°, and 21.4°, respectively), indicating smaller d spacings. The fast Fourier transform (FFT) pattern of the HRTEM image of the HP&HT treated PIC9 sample shows a hexagonal pattern (Figure 3c). With the aid of WAXD data (Figure 4a), the brightest spots were assigned to (111), (220), and (311) planes with calculated d spacings of 0.787, 0.475, and 0.415 nm, respectively (Figure 3c). Moreover, the elongation of the spots in Figure 3c, and the observed closely packed lattice structure (shorter distance between C_{60} molecules) in the WAXD spectrum (Figure 4a), may be due to the probable mixture of unreacted C_{60}, C_{60} dimers, oligomers, and polymers, which causes a distribution of intermolecular spacings. The WAXD spectrum of treated PIC9 sample was fitted by that of an orthorhombic lattice with lattice constants of a = 9.14 Å, b = 9.9 Å, and c = 14.16 Å,[24] in excellent agreement with previous results for HP-produced orthorhombic (polymeric) C_{60}: a = 9.14 Å, b = 9.9 Å, and c = 14.66 Å.[10] These results suggest a fcc to orthorhombic structural change consistent with previous results for C_{60} treated under similar HP&HT conditions.[23,25] The orthorhombic polymeric struc-

dx.doi.org/10.1021/mz400171e | ACS Macro Lett. 2013, 2, 511–517

ture is associated with one-dimensional polymeric C_{60} and indicates that crystals of C_{60} embedded in PI polymerize by the HP&HT treatment. This means that the initial weak van der Waals forces between the C_{60} fillers are replaced by covalent bonds in polymerized C_{60}, and the reinforcement increases. This effect occurs presumably also for smaller entities, like small assemblies or clusters, of C_{60}, giving a range of structures including oligomeric and dimeric C_{60}.

The structural results taken together with previous results for HP&HT neat PI and C_{60} provide three possible sources for the strong reinforcement of the PIC composites: (i) C_{60}–PI covalent bonds, (ii) C_{60} dimers, oligomers, and polymers, and (iii) PI–PI cross-links. In principle, it is possible that the composites have a higher number of PI–PI cross-links than the pure matrix, but the most likely reason for the improvement is a combination of (i) and (ii). That is, C_{60} clusters form dimeric, oligomeric, and polymeric C_{60} in which C_{60} molecules facing PI also form covalent bonds with PI chains, as illustrated schematically in Figure 3g2. Moreover, completely dissolved C_{60} molecules can form single molecule bridges between PI chains (Figure 3g1). It is well-known that the cross-link density of a polymer and the interaction between filler and matrix play important roles in the tensile properties of composites.[7,26] Strong covalent bonding between the filler and matrix provides an effective load transfer interface, which prevents filler pull-out. In this case, the bonds assist the load transfer from PI to the extended C_{60} polymeric structures, which apparently are present in the matrix. As depicted in Figure 5a and b, the

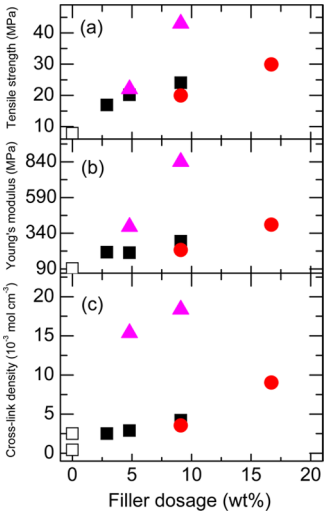

Figure 5. (a) Tensile strength, (b) Young's modulus, and (c) cross-link densities obtained by swelling in toluene plotted against filler content for HP&HT treated: (pink ▲) PIC composite; (black ■, red ●) P- and F-MWCNT filled PI composites from ref 8; and (□) PI from ref 7.

covalently bonded C_{60}/PI composites show better σ_{UTS} and E compared to both 9.1 wt % P-MWCNT and 16.7 wt % F-MWCNT filled PI.[8] This is in correspondence with their higher cross-link densities (Figure 5c), which verifies the importance of the covalently bonded C_{60} for the excellent properties of the composites produced.

The extent of this reinforcement can be estimated using the known reversibility of the C_{60} cross-linking process.[6] Heating at low pressure effectively recovers the initial fcc structure of C_{60} through a kinetically controlled[6,27] process (Supporting Information) and, thus, removes the reinforcement provided by polymerized C_{60} clusters as well as by dimers and oligomers linked to PI only via terminal molecules. Cross-links provided by single C_{60} bridges would probably not be reversible, and these would therefore remain together with the PI–PI cross-links, which are known to be irreversible.

To break C_{60}–C_{60} cross-links, the HP&HT treated PIC9 sample was heated to ~450 K and annealed for 20 h in vacuum (vacuum annealing). After vacuum annealing, the HP&HT treated PIC9 sample showed a 2D partially crystalline microstructure surrounded by amorphous C_{60} (and PI) (Figure 3b), and as marked by the dashed boundaries, the size of the crystalline domains decreased to ~20 nm or less. Moreover, the FFT patterns (Figure 3d and 3e) indicate a less perfect crystalline structure. This suggests that the previously cross-linked C_{60} (dimers, oligomers, orthorhombic, and tetragonal polymer) reverted to individual C_{60} molecules in the form of an amorphous or crystalline (fcc) structure.

Thermal gravimetric analysis (TGA) was also applied to study the depolymerization of C_{60}. As shown in Figure 4c, the TGA curves display a more significant weight decrease for PIC9 than PIC5 between ~450 and 573 K, with an additional decrease by about 2.0 wt % for PIC9 at 523 K (see arrow in Figure 4c). This is in the range of the well-documented depolymerization temperatures of C_{60} dimers and orthorhombic and tetragonal C_{60} near 420, 500, and 550 K, respectively,[10] which indicates that the additional weight decrease of PIC9 was mainly due to loss of individual C_{60} molecules that had depolymerized (see Supporting Information Figure S5). We also measured υ_{swell} and T_2 after the vacuum annealing at 450 K. As depicted in Figure 4b, PI showed an improved strength after vacuum annealing. Although the tensile properties indicate an increase of cross-link density, υ_{swell} decreased slightly from 2.5 × 10^{-3} to 2.03 × 10^{-3} mol cm^{-3}, and T_2 increased slightly to 4.5 × 10^{-4} s. The improved tensile properties may thus be an effect of removal of stresses and defects in the recovered HP&HT treated sample, but the vacuum annealing did not significantly change the microstructure, as shown by the similar ^{1}H solid-state MAS NMR spectra before (Figure 2b, i) and after vacuum annealing (Figure 2b, iii). The result implies that the selected temperature for the vacuum annealing procedure was low enough to avoid extensive scissoring of PI. However, in the case of vacuum-annealed PIC9, υ_{swell} decreased 45%, from 1.84 × 10^{-2} to 1.01 × 10^{-2} mol cm^{-3}, and υ_{swell} of vacuum-annealed PIC5 decreased 25% (from 1.54 × 10^{-2} to 1.16 × 10^{-2} mol cm^{-3}), i.e., less than for PIC9 and in accord with a lower number of C_{60} clusters. Moreover, T_2 of the vacuum-annealed PIC9 increased to 4.5 × 10^{-4} s in agreement with the swelling results of a decreased number of cross-links. (See also the recovered ^{1}H solid-state MAS NMR spectrum, Figure 2b, iv.) The changes of υ_{swell} of the PIC composites are consistent with their tensile performance, as σ_{UTS} of PIC9 decreased by 23%, whereas σ_{UTS} of PIC5 decreased by 15%. As discussed above, HP&HT synthesized PIC9 evidently contained a significant amount of C_{60} clusters, and after vacuum annealing of the PIC composites, the original WAXD spectra (Figure 4a) essentially recovered corroborating that depolymerization of C_{60} caused the decrease of the tensile properties. In fact, despite a likely improved strength of the PI matrix by reduction of stresses and defects, σ_{UTS} and E decreased. On the basis of these data, we can provide a structural model for the cross-linking of C_{60} caused by the HP&HT treatment (Figure 3g) and the subsequent reverse process obtained by vacuum annealing

dx.doi.org/10.1021/mz400171e | ACS Macro Lett. 2013, 2, 511–517

(Figure 3j). The mechanical properties of PIC5 decreased only weakly after vacuum annealing, which shows that it contained mainly irreversible cross-links (PI−PI and PI−C_{60}) and that any depolymerization effect was compensated by an increased strength of the PI matrix. That fewer C_{60} clusters were available for reversible cross-linking is also supported by the weak crystalline features in the WAXD spectra (Figure 4a).

In summary, even though C_{60} is not considered as an ideal additive for tensile reinforcement applications, the results presented here show that C_{60} fillers can provide significantly better reinforcement than CNTs in a network polymer. The origin of this seemingly paradoxial behavior is likely the weak interfacial interaction between CNTs and PI, while in contrast, polymeric C_{60} may have a strong covalently bonded interface with PI. Moreover, C_{60} provides cross-links between PI chains in the form of single C_{60} molecule bridges. Without these bonds, C_{60} fillers do not provide significant reinforcement and should behave similarly to other nonbonded spherical nanoparticles, such as silica, TiO_2 nanoparticles, etc. Thus, reinforcement by C_{60} requires a treatment which induces cycloaddition, and the effects observed here after such treatment suggest that C_{60} can be used as a strong reinforcer and reversible cross-linker in the form of clusters in composite applications based on network polymers. This distinguishes C_{60} from carbon black, which does not form covalent cross-links in rubber composites but instead provides rigidity and reinforcement through the phenomenon of "bound rubber".[28] This nanoscale interfacial interaction, which may be both physical and chemical in nature, is very different from the strong covalent bonds between PI and C_{60}. But most importantly, the reversibility of C_{60}−C_{60} cross-links is very interesting for improved recycling of composite materials. Recycling of rubber-based composite materials (network polymers) is troublesome because of difficulties to break down the chemically cross-linked microstructure.[29] In a polymer composite which is cross-linked only by dimeric or polymeric C_{60}, it would be possible to recycle the polymer matrix as well as a (second) reinforcing system, e.g., one made of carbon fibers, providing both environmental and cost savings. To optimize the system and achieve a fully recyclable composite, one possibility would be to use a starting material consisting of C_{60} dimers in a polymer matrix. Cross-links based entirely on dimers would be fully reversible and strong. Such a reversible curing system would be useful for recycling of both elastomers as well as other cross-linkable polymers. Moreover, the tensile properties of the polymers, e.g., the Young's modulus and maximum extension at break, would be variable via the concentration of dimers.

EXPERIMENTAL SECTION

C_{60} (purity ≥99.9%, MER Corporation) was dispersed in liquid *cis*-1,4-PI (with a number-average relative molecular mass of 38 000, Sigma-Aldrich) using the solvent mixing method.[7,30] Briefly, for a typical 9.1 wt % C_{60}/PI sample, a mixture of 350 mg of C_{60} and 135 mL of toluene (dissolubility of C_{60}: 3.0 mg/mL C_{60} in toluene[31]) was sonicated in a beaker using an ultrasonic pin (VCX130, Sonics & Materials, Inc. USA) at 75% power for 60 min (pulse 20 s on and 10 s off). Subsequently, 3.5 g of PI was added into the beaker, and the sonication continued at 50% power for 120 min (pulse 20 s on and 20 s off). The solvent was thereafter removed under dynamic vacuum at 50 °C until the weight of the mixture did not decrease further, which took ca. 2 days and resulted in a sample with a high viscosity similar to that of the neat polymer. The dried samples were loaded in a cylindrically shaped, custom-made Teflon cell, which was mounted into a piston cylinder apparatus and transferred to a hydraulic press that delivered the load. The pressure was determined from load divided by area with an empirical correction for friction, and the temperature was measured by an internal type K thermocouple. Further details of the experimental setup can be found elsewhere.[32,33] To obtain cross-linked states, the samples were pressurized to 1.5 GPa and then heated to 513 K. The samples were annealed under these conditions for 4 h during which the pressure and temperature were kept constant to within ±1 MPa and ±1 K by two automatic controllers. This HP&HT treatment produced homogeneous plates of cross-linked C_{60}/PI samples (see Supporting Information Figure S3) with a thickness of about 2 mm.

The samples recovered from the Teflon cell after the HP&HT treatment had the form of circular plates. These were cut to dog-bone-shaped pieces by a custom-made die (dimension: 16 mm × 7 mm), and the exact dimensions of the samples were measured by means of a Nikon workshop microscope. These values were used in the calculations of the σ_{UTS} and E (in the range 1−5% strain). Tensile testing of the samples was performed at room temperature using an Instron 3343 tensile tester equipped with a 500 or 1000 N load cell using a testing speed of 10 mm/min. Mass density was measured by the Archimedes' principle by immersion in water at 298 K.

For solid-state MAS NMR experiments, the ground (or highly viscous) material was densely packed into a zirconia MAS rotor with Macor inserts free of carbon for NMR tests. Measurements were carried out on a 400 MHz Infinity spectrometer (Chemagnetics, USA) with a 4 mm double resonance CP MAS probe. ^{13}C CP MAS NMR experiments were acquired under strong proton decoupling using a contact time of 1−10 ms duration (1, 5, and 10 ms) and, normally, a repetition delay of 6 s at a MAS speed of 10 kHz. The ^{13}C NMR spectra were assigned using adamantane as an external standard.

The HRTEM samples were cut by a Leica Reichert Ultracuts ultramicrotome equipped with a diamond knife and subsequently placed on copper slot grids. HRTEM (JEOL JEM-2200FS) was used for imaging ultrathin sections (ca. 50 nm in thickness) of samples at 200 KV. FFT patterns were obtained by converting typical TEM images.

WAXD was carried out using a Siemens/Bruker D5000 diffractometer with Cu Kα radiation at an acceleration voltage of 40 kV and a tube current of 30 mA. TGA was performed on a Mettler-Toledo DSC-1 start system with a scan rate of 5 K per min from 298 to 973 K under a nitrogen flow. The samples (ca. 15 mg for each sample) were ground into powder and heated in alumina open crucibles with 70 mL capacity.

Cross-link densities were determined using the swelling method (υ_{swell}). The samples were immersed in *n*-heptane or toluene at room temperature for 48 h,[30] and υ_{swell} was estimated by the Flory−Rehner equation,[34,35] as described in detail previously.[8,30] Cross-link densities were also determined from the results of the E (υ_E) and NMR measurements (υ_{NMR}), as described previously.[8] The densities of the composites, which were used for calculation of υ_E and υ_{NMR}, are shown in Supporting Information Figure S4.

ASSOCIATED CONTENT

Supporting Information

Mechanical properties of carbon black filled PI, NMR spectra of untreated/treated PIC9 samples at various contact times and MAS speeds, TEM image, and densities of PIC samples. This material is available free of charge via the Internet at http://pubs.acs.org.

AUTHOR INFORMATION

Corresponding Author

*E-mail: ove.andersson@physics.umu.se.

Notes

The authors declare no competing financial interest.

■ ACKNOWLEDGMENTS

We are grateful for financial support from Magn. Bergvalls foundation, Kungl. Vetenskapsakademiens fonder, and the Swedish Research Council. We thank Dr. Patrik Fernberg for helpful discussions.

■ REFERENCES

(1) Novoselov, K. S.; Geim, A. K.; Morozov, S. V.; Jiang, D.; Zhang, Y.; Dubonos, S. V.; Grigorieva, I. V.; Firsov, A. A. *Science* **2004**, *306*, 666.
(2) Iijima, S. *Nature* **1991**, *354*, 56.
(3) Iijima, S.; Ichihashi, T. *Nature* **1993**, *363*, 603.
(4) Kroto, H. W.; Heath, J. R.; O'Brien, S. C.; Curl, R. F.; Smalley, R. E. *Nature* **1985**, *318*, 162.
(5) Editorial. *Nat. Nano* **2010**, *5*, 691.
(6) Sundqvist, B. *Adv. Phys.* **1999**, *48*, 1.
(7) Tonpheng, B.; Yu, J.; Andersson, B. M.; Andersson, O. *Macromolecules* **2010**, *43*, 7680.
(8) Yu, J.; Tonpheng, B.; Gröbner, G.; Andersson, O. *Macromolecules* **2012**, *45*, 2841.
(9) Tonpheng, B.; Andersson, O. *Eur. Polym. J.* **2008**, *44*, 2865.
(10) Sundqvist, B. Polymeric Fullerene Phases Formed Under Pressure. In *Fullerene-Based Materials*; Springer: Berlin/Heidelberg, 2004; Vol. *109*, pp 85.
(11) Nielsen, L. E.; Landel, R. F. *Mechanical tests and polymer transitions*, 2nd ed.; Marcel Dekker: New York, 1994.
(12) Kropka, J. M.; Garcia Sakai, V.; Green, P. F. *Nano Lett.* **2008**, *8*, 1061.
(13) Kropka, J. M.; Putz, K. W.; Pryamitsyn, V.; Ganesan, V.; Green, P. F. *Macromolecules* **2007**, *40*, 5424.
(14) Tuichiev, S.; Tabarov, S.; Ginzburg, B. *Tech. Phys.* **2008**, *53*, 956.
(15) Wu, C.-S. *J. Appl. Polym. Sci.* **2010**, *115*, 3489.
(16) Tycko, R.; Haddon, R. C.; Dabbagh, G.; Glarum, S. H.; Douglass, D. C.; Mujsce, A. M. *J. Phys. Chem.* **1991**, *95*, 518.
(17) Johnson, R. D.; Meijer, G.; Bethune, D. S. *J. Am. Chem. Soc.* **1990**, *112*, 8983.
(18) Yang, C.; Hu, J. G.; Heeger, A. J. *J. Am. Chem. Soc.* **2006**, *128*, 12007.
(19) Buzaré, J.-Y.; Silly, G.; Emery, J.; Boccaccio, G.; Rouault, E. *J. Appl. Polym. Sci.* **2003**, *87*, 3.
(20) Spiess, H. W. *Chem. Rev.* **1991**, *91*, 1321.
(21) In the virgin PIC9 composite, the solid-state MAS CP spectrum (contact time: 10 ms) shows a small peak at 143 ppm due to C_{60}. Since C_{60} has no attached protons it must become polarized from protons in its immediate neighborhood, as observed in other C_{60}−polymer mixtures despite that C_{60} was not covalently bonded to the polymer (see Supporting Information Figure S2).
(22) Scanlon, J. C.; Ebert, L. B. *J. Phys. Chem.* **1993**, *97*, 7138.
(23) Blank, V. D.; Buga, S. G.; Dubitsky, G. A.; Serebryanaya, N. R.; Popov, M. Y.; Sundqvist, B. *Carbon* **1998**, *36*, 319.
(24) The spectrum of the HP&HT-treated PIC9 sample was fitted by Chekcell software in an orthorhombic lattice.
(25) Marques, L.; Hodeau, J. L.; Núñez-Regueiro, M.; Perroux, M. *Phys. Rev. B* **1996**, *54*, R12633.
(26) Frankland, S. J. V.; Caglar, A.; Brenner, D. W.; Griebel, M. *J. Phys. Chem. B* **2002**, *106*, 3046.
(27) Nagel, P.; Pasler, V.; Lebedkin, S.; Soldatov, A.; Meingast, C.; Sundqvist, B.; Persson, P. A.; Tanaka, T.; Komatsu, K.; Buga, S.; Inaba, A. *Phys. Rev. B* **1999**, *60*, 16920.
(28) Dannenberg, E. M. *Rubber Chem. Technol.* **1986**, *59*, 512.
(29) Yamazaki, H.; Nagasawa, T.; Choi, W.; Endo, T. *J. Appl. Polym. Sci.* **2006**, *101*, 4003.
(30) Tonpheng, B.; Yu, J.; Andersson, O. *Macromolecules* **2009**, *42*, 9295.
(31) Kulkarni, P. P.; Jafvert, C. T. *Environ. Sci. Technol.* **2007**, *42*, 845.
(32) Yu, J.; Tonpheng, B.; Gröbner, G.; Andersson, O. *Carbon* **2011**, *49*, 4858.
(33) Yu, J.; Tonpheng, B.; Andersson, O. *Macromolecules* **2010**, *43*, 10512.
(34) Flory, P. J.; John Rehner, J. *J. Chem. Phys.* **1943**, *11*, 512.
(35) Flory, P. J. *J. Chem. Phys.* **1950**, *18*, 108.